Multicomponent Diffusion in Molten Slags

M.D. DOLAN and R.F. JOHNSTON

A method for investigating the diffusion of metal cations in multicomponent slag systems was developed. This method used microprobe analysis and allowed the analysis of the diffusion of multiple species within a single system. This project focused on the diffusion behavior of manganese, iron, calcium, and silicon in silicate slags, in order to simulate industrial steel and ferromanganese production. The molecular structure of CaO-Al_2O_3-SiO_2 slags was investigated with Raman spectroscopy, and oxidation states of manganese and iron in slags of varying composition were determined. This study identified the variation in diffusivity of slag components with changes in composition and temperature of multicomponent slag systems. An empirical model based on the correlation between optical basicity and diffusivity was developed to predict the multicomponent diffusivity of ionic species in molten silicate slags. The model takes into account properties of the bulk slag and the network forming ability of the diffusing species. The relative rate of diffusion of metal cations is proportional to the optical basicity coefficient of that species, while the rate of diffusion of all species increases exponentially with the calculated optical basicity of the bulk slag.

I. INTRODUCTION

SINCE the article by Towers *et al.*[1] on the diffusion of Ca^{2+} in molten CaO-SiO_2 slags, many studies employing the radiotracer method (for example, References 2 through 8) have been devoted to the diffusion of ionic and molecular species through molten slags and glasses. However, many aspects of this field of study are still unexamined. This project aims to enhance current knowledge by providing a comprehensive understanding of the diffusion of metals cations (including transition metals) and silicon (as silicate anions) in multicomponent systems.

Transport processes and kinetics of interphase reactions determine the rate of production in a smelting system. Because the diffusivity of an element through liquid metal is shown to be approximately an order of magnitude greater than diffusivity of the same element through liquid slag,[9] diffusion through the slag phase is a rate-limiting step in the overall process. Consequently, studying the rate of diffusion of manganese and iron through the slag phase is important in determining kinetics of the smelting processes.

Tracer studies only apply to the limiting case in which the concentration gradient of all nontracer species is zero. Once a significant concentration gradient of a second species is introduced, cross-effects from one species impart a flux on other diffusing species, causing a departure from the ideal tracer diffusivity to multicomponent diffusivity. Because industrial smelting systems are complex, with multiple species and multiple concentration gradients, evaluation of the cross-effects between slag components is necessary.

The diffusivity of manganese, iron, calcium, and silicon will be thoroughly investigated, in slags of varying composition and temperature, in multicomponent systems in which more than one concentration gradient exists. Varying the concentration gradients of different species will allow the calculation of multicomponent diffusion coefficients. Additionally, the study will include analysis of slag structure by Raman spectroscopy and a determination of the oxidation states of manganese and iron in slags of varying composition.

The concept of optical basicity, introduced by Duffy and Ingram[10] for characterization of glasses, has been used to correlate slag composition with capacities, activities, and redox equilibria. Most recently, the concept has been applied to viscosity modeling.[11] Table I shows values of optical basicity coefficients (Λ) for various oxides, calculated using Pauling electronegativities and average electron density, published by Sommerville and Yang.[12]

Each oxidation state of a transition metal has a different ability to integrate with the silicate network, and as such, the influence of transition metals on slag basicity, when there are multiple oxidation states present, is not fully defined. Sosinsky and Sommerville[13] found a correlation between optical basicity and sulfide capacity. This relation can be correlated to slags containing transition metals to give an "apparent optical basicity." These apparent optical basicity values for transition metals will be investigated as suitable correlating properties for results herein.

II. RAMAN SPECTROSCOPY OF SLAGS

Raman spectroscopy has been used as an analytical tool for pure and simple silicates for many years. As such, the peaks for silicate structural units are generally well defined. Depending on the content of other oxides, silicates generally consist of a mixture of monomer species (SiO_4^{4-}), chains (*e.g.,* $Si_2O_6^{4-}$), sheet units (*e.g.,* $Si_2O_5^{2-}$), and tetrahedral SiO_2 and AlO_2^-.[14,15,16] As the nature of the Si-O covalent bonds changes with each of these formations, each has a distinct emission peak. The radial distribution function for quenched glass is almost identical to that of molten glass;[14] therefore, quenched samples were used to describe the structure of molten samples.

M.D. DOLAN, Postdoctoral Associate, is with the Department of Ceramic Engineering and Materials Science, New York State College of Ceramics at Alfred University, Alfred, NY 14802. Contact e-mail: dolanm@alfred.edu R.F. JOHNSTON, Deputy Head of School (Projects), is with the School of Business and Technology, La Trobe University, Bendigo, Victoria 3552, Australia.

Manuscript submitted June 16, 2003.

$CaO-Al_2O_3-SiO_2$ slags of varying composition were prepared from high-purity reagents. Raw materials were roasted at 1000 °C for 24 hours to remove volatile materials, and then fused at 1500 °C under vacuum for 5 hours. The melt was quenched, finely ground, and fused once more and quenched to give a homogeneous degassed glassy sample.

Slag compositions, and a summary of spectral information, are listed in Table II. The range of compositions should give structural information of SiO_2, with (1) changing CaO content and (2) changing Al_2O_3 content. Basicity is calculated according to the optical basicity method.[12]

Figures 1 and 2 show the high-frequency envelope of the Raman emission spectra for the highest and lowest basicity slags, respectively. The low-frequency envelope has been ignored here, as the high-frequency envelope provides adequate information regarding structural detail.

The frequencies of given silicate anions are constant to within about 15 cm^{-1} across the range of compositions. These peaks are in approximately the same range as those found by Mysen *et al.*[14] All four silicate anions, and SiO_2 and AlO_2^- tetrahedra, were present simultaneously in all compositions. The position of these coupled peaks was constant around 1005 and 1110 cm^{-1}. This is a departure from the results observed by Mysen *et al.,* where these peaks were shifted to lower frequencies with increasing aluminum concentration. The lower coupled SiO_2-AlO_2^- peak had a much stronger intensity, between 2 and 5 times greater, in all compositions. As the CaO content increased, the relative amount of smaller structural units (monomer, dimer, chain) increased. As the CaO content increased, the relative amounts of SiO_2 and AlO_2^- decreased. As the Al_2O_3 content increased at constant silica constant, the relative intensity of the coupled SiO_2-AlO_2^- peaks increased.

Table I. Recommended Optical Basicity (Λ) Values for Various Oxides

K_2O	Na_2O	BaO	Li_2O	SrO	CaO	MnO	FeO
1.40	1.20	1.10	1.05	1.05	1.00	0.95	0.92
MgO	Cr_2O_3	Fe_2O_3	Al_2O_3	TiO_2	SiO_2	B_2O_3	P_2O_5
0.85	0.69	0.69	0.65	0.65	0.48	0.42	0.40

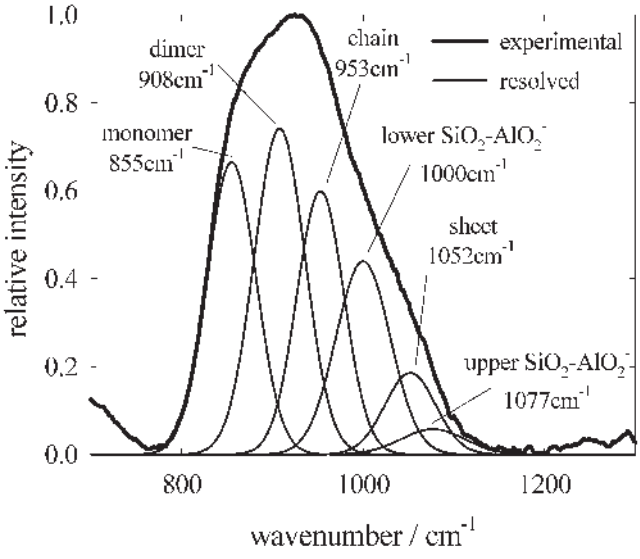

Fig. 1—High-frequency Raman spectrum of $54CaO-6Al_2O_3-40SiO_2$, showing resolved bands for component silicate structures.

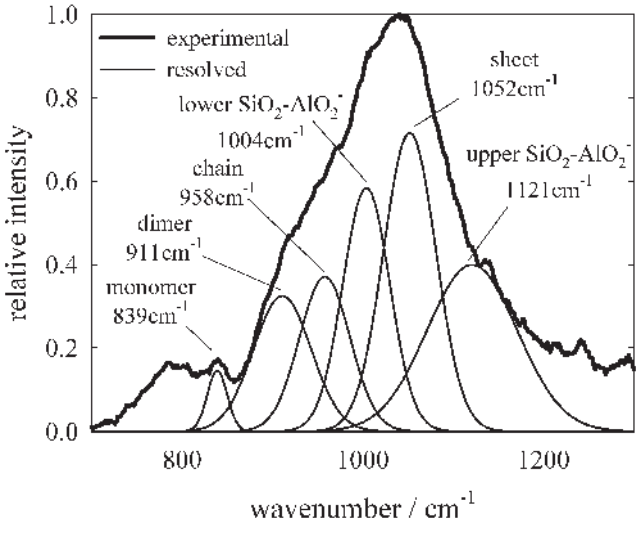

Fig. 2—High-frequency Raman spectrum of $22CaO-6Al_2O_3-72SiO_2$, showing resolved bands for component silicate structures.

Table II. Summary of Resolved Raman Spectra for $CaO-Al_2O_3-SiO_2$ Slags*

		54-6-40	45-12-43	33-15-52	37-11-52	42-6-52	26-9-66	13-15-72	22-6-72
Monomer	Mean	855	853	842	845	845	840	846	839
	amplitude	45	25	6	4	7	4	4	4
Dimer	Mean	908	908	905	905	903	912	910	911
	amplitude	52	53	38	34	46	18	44	26
Chain	Mean	953	955	956	955	957	958	958	958
	amplitude	39	38	44	42	50	25	37	26
Sheet	Mean	1052	1052	1053	1056	1055	1054	1046	1052
	amplitude	13	16	38	31	36	49	54	52
Tetrahedral (lower)	Mean	1000	1000	1004	1008	1008	1008	1000	1004
	amplitude	33	42	48	58	51	47	37	38
Tetrahedral (upper)	Mean	1077	1077	1105	1105	1103	1125	1110	1121
	amplitude	5	9	17	19	8	43	14	50

*Slag compositions, expressed as molar percentages, are shown in the top line of the table. Peak amplitudes are dimensionless. Positions of peak means are expressed in terms of wavenumbers.

III. OXIDATION STATES OF IRON AND MANGANESE

The oxidation states of managanese and iron in experimental slags were determined by titration and spectroscopy. Powdered slag was digested in hydrofluoric acid under nitrogen. Total iron was determined by atomic absorption spectroscopy (AAS), while ferrous iron was determined volumetrically by titration with dichromate. Total manganese was determined spectroscopically by conversion to permanganate, and manganic manganese was determined by reaction with a standard Fe^{2+} solution, followed by titration against dichromate to determine residual iron.

Results for oxidation state determinations for manganese and iron in $CaO\text{-}Al_2O_3\text{-}SiO_2$ slags are shown in Figure 3. The ratio M^{3+}/M^{2+} for both species follows an exponential growth with increasing slag basicity. There is large experimental error, particularly at higher M^{3+}/M^{2+} values, due to the experimental technique involved. The results are similar to published results.[17,18]

The oxidation state of iron is dependent on oxygen partial pressure. Slags equilibrated in air at atmospheric pressure have a higher proportion of Fe^{3+} at any given basicity. At an oxygen partial pressure of 0.002 atm and basicity of 0.57, iron is almost exclusively in the II state. The proportion of the III state increases as slag basicity increases. At an optical basicity of 0.68, the Fe^{3+}/Fe^{2+} ratio is approximately 0.3.

At an oxygen partial pressure of around 0.002 atm and basicity between 0.57 and 0.65, manganese is almost exclusively in the II state. At a basicity of 0.68, the Mn^{3+}/Mn^{2+} ratio is about 0.15.

IV. DIFFUSION METHOD

Multicomponent diffusion experiments were conducted in three, four, and five $(N + 1)$ component systems, comprising (N) solutes (diffusing species). Solvent species are considered to be those species not diffusing. In all experiments, the solvent comprises aluminum oxide and free oxygen ions, and other species with no concentration gradient in that particular experiment. Systems studied were the following:

1. Three component—diffusion of two species (manganese and iron/calcium/silicon) in solvent ($CaO\text{-}Al_2O_3\text{-}SiO_2\text{-}MnO\text{-}FeO_x$ slags);
2. Four component—diffusion of three species (calcium, silicon, and manganese) in a solvent ($CaO\text{-}Al_2O_3\text{-}SiO_2\text{-}MnO$ slags); and
3. Five component—diffusion of four species (calcium, silicon, manganese, and iron) in a solvent ($CaO\text{-}Al_2O_3\text{-}SiO_2\text{-}MnO\text{-}FeO_x$ slags).

Experiments were conducted under conditions of varying composition and temperature. In all experiments, the concentration gradient of aluminum oxide was kept as close to zero as possible.

Multicomponent diffusion coefficients, D_{ij}, were calculated according to Eq. [1].

$$J_v^i = -\sum_{i=1}^{N} D_{ij}^v \frac{dC_j}{dx} \quad (i = 1, 2 \ldots N) \qquad [1]$$

The term J is the flux of species i, N is the number of diffusing species, D_{ij} is the diffusion coefficient of species i induced by the concentration gradient in species j.[19] The term "multicomponent" refers to simultaneous diffusion of multiple species and not the number of oxides in the given slag.

The semi-infinite capillary method was employed, in which a 2-mm internal diameter capillary containing a given slag was immersed in a larger reservoir of a different slag. Base slags were prepared from high-purity SiO_2, $CaCO_3$, and Al_2O_3. Compositions are listed in Table III. Slags are characterized by optical basicities of the $CaO\text{-}Al_2O_3\text{-}SiO_2$ base slag, per Sommerville and Yang.[12] Fe_2O_3 and MnO_2 were added as required to give the desired concentration gradients. Powders were blended to the required compositions and calcined at 1000 °C for 24 hours, then heated to 1500 °C for several hours under vacuum, cooled, quenched, and ground to ensure homogeneity. Capillaries were filled using pressure difference.

Filled capillaries were suspended into a platinum crucible containing powdered slag of the necessary composition. The system was placed into an argon-filled tube furnace heated to the desired temperature. After the desired time elapsed, the crucible was removed from the furnace and air-quenched. Experimental diffusion time commenced when the thermocouple temperature reached 50 °C below the temperature of the experiment. All experiments were conducted at 1500 °C unless otherwise stated. Capillaries were mounted in resin or

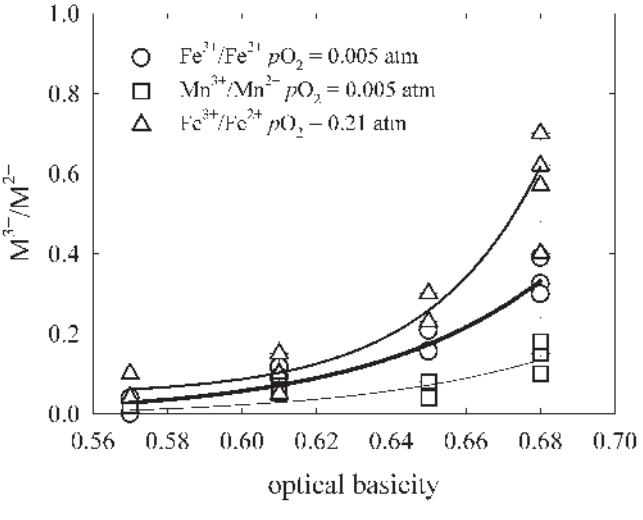

Fig. 3—Relative proportions of II and III states for (1) manganese equilibrated at $pO_2 = 0.002$ atm and (2) iron equilibrated at (2) $pO_2 = 0.002$ atm and (3) 0.21 atm.

Table III. Compositions of Experimental Slags in Terms of Weight Percentages and Optical Basicity (Λ)

Slag	Pct SiO_2	Pct CaO	Pct Al_2O_3	Λ
1	62.0	23.5	14.5	0.57
2	55.0	28.5	16.5	0.59
3	48.5	33.0	18.5	0.61
4	40.0	40.0	20.0	0.65
5	39.0	51.0	10.0	0.68

bakelite and polished to reveal a longitudinal cross section. The concentrations of each species were measured along the length of the capillary using electron or X-ray microprobes at about 0.01-mm intervals. Capillaries containing bubbles were discarded.

Figure 4 shows a sample five-component diffusion experiment, in which manganese, iron, calcium, and silicon are the diffusing species. Equation [2] gives the concentration profile of each element in terms of effective diffusion coefficient D_e, a single term that is the sum of all individual multicomponent contributions.

$$\frac{(C - C_S)}{(C_0 - C_S)} = \text{erfc}\,\frac{x}{2\sqrt{D_e t}} \qquad [2]$$

The term C_S is the crucible concentration, C_0, is the initial capillary concentration, x is distance from the capillary/crucible junction, C is the concentration at any point x along the dimension of diffusion, and t is time.[19]

The following assumptions are made.

1. Diffusion is single dimensional.
2. There are no wall effects. This was verified by determining concentrations across the capillary.
3. The concentration at the crucible/capillary junction is constant.
4. There are no convection currents in the capillary. This is achieved through maintaining a temperature gradient and placing the densest slag in the crucible.

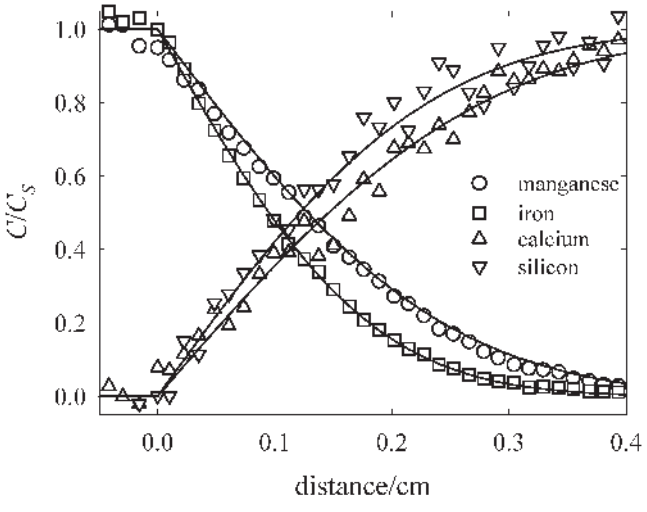

Fig. 4—Concentration profiles of manganese, iron, calcium, and silicon from a five-component experiment, fitted by Eq. [2].

The effective diffusion coefficient for each diffusing species was determined by applying Eq. [2] to the experimental data using a nonlinear fitting routine. The flux of each species through the interface ($x = 0$) was calculated using the effective diffusion coefficient and Fick's first law.[19] The concentration gradient was taken as the concentration difference across the interface at $t \to 0$, in units of mole/g.

V. DIFFUSION RESULTS

A. *Three Component Systems*

Effective diffusivities for the three-component Mn-Fe system are shown in Table IV. Results are virtually identical in all but the most basic slag, in which $D_{e,\text{Mn}} > D_{e,\text{Fe}}$. Effective diffusivities for the three-component Mn-(Ca/Si) systems are shown in Table V. Results follow the trend $D_{e,\text{Ca}} > D_{e,\text{Mn}} > D_{e,\text{Si}}$.

Varying the concentration of manganese and iron (by equal amounts) from 2 to 5 to 10 wt pct yielded the same coefficient of diffusion. Although diffusion coefficients are not independent of concentration, any variation in diffusivity has been shown to be negligible. Concentration does significantly alter diffusivity in other respects. Increasing the concentration of a diffusing species alters the composition (and viscosity) of the slag, which in turn alters the coefficient of diffusion. Also, increasing the concentration of a given species alters the concentration gradient of other species. An increase in silicon concentration gradient has a significant effect. The combination of composition changes and cross-effects outlined previously far outweighs any influence arising from concentration dependence.

Iron and manganese will have very similar diffusion properties, because both have very similar chemical and physical properties. Since this is the case, increasing the respective concentration gradients by an equal amount should not increase the flux ratio between the two. In addition, the three-component ferrous system has a relatively high electrical

Table IV. Diffusivities of Manganese and Iron in Three-Component Systems at 1500 °C

Optical Basicity	$D_{e,\text{Mn}}/(10^{-6}\ \text{cm}^2\ \text{s}^{-1})$	$D_{e,\text{Fe}}/(10^{-6}\ \text{cm}^2\ \text{s}^{-1})$
0.68	4.8 ± 0.7, 5.2 ± 0.8, 4.3 ± 0.6, 4.7 ± 0.7	3.8 ± 0.6, 4.2 ± 0.6, 4.3 ± 0.6
0.65	2.9 ± 0.4, 3.2 ± 0.5, 2.9 ± 0.4, 2.9 ± 0.4	3.1 ± 0.4, 3.0 ± 0.4, 2.9 ± 0.5,
0.61	1.8 ± 0.3, 1.9 ± 0.3	1.9 ± 0.3, 1.7 ± 0.3

Table V. Diffusivities of Manganese, and Calcium or Silicon, in Three-Component Systems at 1500 °C

System	Optical Basicity	$D_{e,\text{Mn}}/(10^{-6}\ \text{cm}^2\ \text{s}^{-1})$	$D_{e,\text{Ca}}/(10^{-6}\ \text{cm}^2\ \text{s}^{-1})$	$D_{e,\text{Si}}/(10^{-6}\ \text{cm}^2\ \text{s}^{-1})$
Mn-Ca	0.65	2.6 ± 0.4, 3.4 ± 0.5	3.2 ± 0.5, 3.5 ± 0.5	
Mn-Si	0.65	2.6 ± 0.4, 2.4 ± 0.4		1.9 ± 0.3, 2.2 ± 0.3
Mn-Ca	0.68	4.3 ± 0.6, 4.7 ± 0.7	4.9 ± 0.7, 5.2 ± 0.8	
Mn-Si	0.68	4.6 ± 0.7, 4.7 ± 0.7		2.7 ± 0.4, 3.1 ± 0.5

Table VI. Diffusivities of Manganese and Calcium in Four-Component Systems, and Silicon in Four- and Five-Component Systems, at 1500 °C

Optical Basicity	$D_{e,Mn}/(10^{-6}\ cm^2\ s^{-1})$	$D_{e,Ca}/(10^{-6}\ cm^2\ s^{-1})$	$D_{e,Si}/(10^{-6}\ cm^2\ s^{-1})$
0.68	4.3 ± 0.6, 5.0 ± 0.8, 3.2 ± 0.5, 4.3 ± 0.6	5.4 ± 0.8, 5.7 ± 0.9, 6.0 ± 0.9, 6.5 ± 1.0	2.9 ± 0.4, 2.9 ± 0.4, 2.9 ± 0.4, 4.3 ± 0.6
0.65	2.6 ± 0.4, 2.3 ± 0.3, 2.5 ± 0.4, 2.8 ± 0.5	3.7 ± 0.6, 3.4 ± 0.5, 3.6 ± 0.5	1.4 ± 0.2, 1.5 ± 0.2, 1.8 ± 0.3, 1.6 ± 0.2, 1.5 ± 0.2, 2.4 ± 0.4
0.61	1.5 ± 0.2, 1.4 ± 0.2, 1.4 ± 0.2	1.6 ± 0.2, 3.1 ± 0.5, 2.4 ± 0.4, 2.3 ± 0.3	1.5 ± 0.2, 1.2 ± 0.2, 1.1 ± 0.2, 1.6 ± 0.2, 1.2 ± 0.2
0.59	1.3 ± 0.1, 1.0 ± 0.1	2.5 ± 0.4, 2.7 ± 0.4	2.3 ± 0.3
0.57	0.8 ± 0.1, 0.6 ± 0.1	1.3 ± 0.2, 1.5 ± 0.2	1.0 ± 0.2, 0.6 ± 0.1, 1.2 ± 0.2

conductivity,[20,21] meaning regions of electric charge will not readily develop.

Considering these two factors, it can be stated that diffusion values for manganese and iron in three-component systems are equal to the values of D_{MnMn} and D_{FeFe}, respectively for any slag with an equivalent basicity.

Three-component experiments involving diffusion of calcium and manganese in a nonferrous slag reveal the magnitude of the cross-effect induced by the calcium concentration gradient on the flux of manganese (D_{MnCa}). Because this value was determined in a nonferrous slag, it will also be applicable to the four-component system. These results are small compared to experimental error, and are probably not significant when other greater cross-effects are considered.

Three-component experiments involving diffusion of silicon and manganese can be used to determine the value of D_{MnSi}. The value of D_{MnSi} is far greater than D_{MnCa}. In the Ca-Mn system, the cross-effect of calcium on manganese will be approximately equal to the cross-effect of manganese on calcium, because both species are discrete cations of similar size with a 2+ charge. Therefore, $D_{CaMn} \approx D_{MnCa}$.

In the case of manganese and silicon, there is a significant size difference between $Mn^{2+/3+}$ and silicate anions, meaning the relative force applied on silicon by manganese is much less than that of silicon on manganese. Because the Ca-Mn cross-effect has been shown to be very small, that of the metal cations on silicon will be smaller still. As such, it is reasonable, considering the errors involved, to set these values to zero.

Therefore, $D_{SiMn} = D_{SiFe} = D_{SiCa} = 0$.

As the cross-effects on silicon have been set to zero, regardless of system, the diffusivity of silicon is equal to the value of D_{SiSi}. Therefore, $D_{e,}Si = D_{SiSi}$.

B. *Four-Component Systems*

Four-component experiments featured manganese diffusing into the capillary, and calcium and silicon diffusing out of the capillary. Effective diffusivities for four-component Mn-Si-Ca systems are shown in Table VI. Results follow the trend $D_{e,Ca} > D_{e,Mn} > D_{e,Si}$. The four-component system featured diffusion of manganese opposed by diffusion of calcium and silicon. Because the values of D_{MnMn} at all basicities are known from three-component experiments, the magnitude of the silicon cross-effects on silicon can be determined at all basicities. The decrease in diffusivity of manganese with the application of a silicon gradient is approximately uniform across the range of basicities.

Table VII. Diffusivities of Manganese and Iron in Five-Component Systems at 1500 °C

Optical Basicity	$D_{e,Mn}/(10^{-6}\ cm^2\ s^{-1})$	$D_{e,Fe}/(10^{-6}\ cm^2\ s^{-1})$
0.68	3.5 ± 0.5, 3.2 ± 0.5	2.6 ± 0.4, 2.8 ± 0.4
0.65	2.3 ± 0.3	1.4 ± 0.2
0.61	1.2 ± 0.2, 1.4 ± 0.2	0.7 ± 0.1, 0.9 ± 0.1
0.57	0.7 ± 0.1, 0.3 ± 0.1	0.2 ± 0.1, 0.2 ± 0.1

Table VIII. Diffusion Coefficient Matrix for the Four-Component Mn-Ca-Si System, with an Optical Basicity of 0.65 and Temperature of 1500 °C, with $D_{ij}/(10^{-6}\ cm^2\ s^{-1})$

D_{MnMn}	3.0 ± 0.5	D_{CaMn}	0.2 ± 0.1	D_{SiMn}	0.0 ± 0.1
D_{MnCa}	0.2 ± 0.1	D_{CaCa}	4.0 ± 0.8	D_{SiCa}	0.0 ± 0.1
D_{MnSi}	1.0 ± 0.2	D_{CaSi}	1.0 ± 0.3	D_{SiSi}	1.7 ± 0.4

The magnitude of the Ca-Mn cross-effect is expected to remain small. If this value remains constant across the basicity range at $0.1 \times 10^{-6}\ cm^2\ s^{-1}$, D_{MnSi} can be calculated for all basicities.

C. *Five-Component Systems*

Five-component experiments featured manganese and iron diffusing into the capillary, and calcium and silicon diffusing out of the capillary. Effective diffusivities for Mn and Fe in five-component Mn-Fe-Ca-Si systems are shown in Table VII. Results follow the trend $D_{e,Mn} > D_{e,Fe}$. Effective diffusivities for silicon are displayed in Table V. Because $D_{e,Si}$ is equal to D_{SiSi}, differentiation between four- and five-component diffusivities is not necessary.

The five-component experiments featured diffusion of manganese, iron, silicon, and calcium simultaneously. Because the slags contained iron, electrical conductivity will be relatively high, and for reasons discussed previously, the only significant cross-effect will be that induced by silicon onto the metal cations.

As the silicon gradient is effectively doubled compared to the four-component experiments, the diffusivity of manganese at all basicities is lower than the corresponding four-component experiment. Once more the D_{MnMn} and

Table IX. Diffusion Coefficient Matrix for the Five-Component Mn-Fe-Ca-Si System, with an Optical Basicity of 0.65 and Temperature of 1500 °C, with $D_{ij}/(10^{-6}\text{cm}^2\,\text{s}^{-1})$

D_{MnMn}	3.0 ± 0.5	D_{FeMn}	0.0 ± 0.1	D_{CaMn}	0.0 ± 0.1	D_{SiMn}	0.0 ± 0.1
D_{MnFe}	0.0 ± 0.1	D_{FeFe}	2.9 ± 0.5	D_{CaFe}	0.0 ± 0.1	D_{SiFe}	0.0 ± 0.1
D_{MnCa}	0.0 ± 0.1	D_{FeCa}	0.0 ± 0.1	D_{CaCa}	3.7 ± 0.7	D_{SiCa}	0.0 ± 0.1
D_{MnSi}	0.9 ± 0.4	D_{FeSi}	1.5 ± 0.4	D_{CaSi}	0.7 ± 0.5	D_{SiSi}	1.8 ± 0.5

Table X. Diffusivities of Manganese and Iron in Systems with an Optical Basicity 0.61, at Temperatures between 1400 °C and 1600 °C

	Three Component	Three Component	Four Component
T/°C	$D_{e,Mn}/(10^{-6}\text{ cm}^2\text{ s}^{-1})$	$D_{e,Fe}/(10^{-6}\text{ cm}^2\text{ s}^{-1})$	$D_{e,Mn}/(10^{-6}\text{ cm}^2\text{ s}^{-1})$
1400	1.3 ± 0.2, 0.8 ± 0.1	1.3 ± 0.2, 0.9 ± 0.1	0.6 ± 0.1, 0.2 ± 0.1
1450			0.9 ± 0.1
1500	1.8 ± 0.3, 1.9 ± 0.3	1.7 ± 0.3, 1.9 ± 0.3	1.5 ± 0.2, 1.4 ± 0.2, 1.4 ± 0.2
1550			2.1 ± 0.2
1600	3.0 ± 0.5, 3.5 ± 0.6	2.8 ± 0.4, 3.2 ± 0.5	2.3 ± 0.3, 2.3 ± 0.3

five-component diffusivities vary by an approximately equal amount across the range of basicities.

The diffusivity of iron follows a similar exponential relationship with optical basicity to that of manganese. At all basicities studied, the diffusivity of iron was less than that of manganese in the presence of a silicon gradient.

D. *Diffusion Coefficient Matrices*

Multicomponent diffusion coefficients can be presented in a diffusion-coefficient matrix. For a system with $N + 1$ species (one solvent and N solutes), there are N^2 diffusion coefficients to describe the system.

Multicomponent diffusion coefficient matrices can be constructed for the four- and five-component systems. The diffusion coefficient matrix for the four-component CaO-SiO_2-MnO system at basicity 0.65 and 1500 °C is shown in Table VII. The diffusion coefficient matrix for the five-component CaO-SiO_2-MnO-FeO_x system at basicity 0.65 and 1500 °C and basicity of 0.65 is shown in Table IX.

E. *Effect of Temperature*

Three-component and four-component experiments were conducted with a basicity of 0.61 and temperatures ranging from 1400 °C to 1600 °C. Diffusivities of manganese and iron are shown in Table X. Calculated activation energies of diffusion (E_D), which range between 140 and 175 kJ mol^{-1} for the three systems studied, are shown in Table XI.

According to Turkdogan,[17] activation energies for each of these phenomena in a particular slag type follow the general trend $E_\eta > E_D > E_\kappa$, where η is viscosity and κ is conductivity. Values for E_η in CaO-SiO_2 slags typically fall in the range 200 to 300 kJ mol^{-1}.[5] The National Physics Laboratory (NPL) model[11] predicts the activation energy of viscous flow for the experimental slag with an optical basicity of 0.61 to be 190 kJ mol^{-1}, with an error of around 20 pct. At 1600 °C, E_κ varies from 180 kJ mol^{-1} at 0.2CaO-SiO_2 to 85 kJ mol^{-1} at 0.6CaO-SiO_2.[17] The E_D values fall into a range expected from conductivity and viscosity measurements; it can be stated that the diffusion data obtained are in an acceptable range and the results are relevant. If

Table XI. Calculated Activation Energies of Diffusion for Manganese and Iron in Systems with an Optical Basicity of 0.61

System	E_D/kJ mol^{-1}
four-component Mn	175 ± 20
three-component Mn	150 ± 20
three-component Fe	140 ± 20

E_D differed markedly from the suggested trend, questions could be raised regarding the validity of the data.

While bearing in mind that this study samples a small composition range compared to the NPL model, the calculated activation energies of diffusion and the NPL activation energy of viscosity are almost identical. Because Arrhenian behavior has been demonstrated by the NPL model to apply to slag viscosity, it follows that diffusivity will also follow Arrhenian behavior. As the activation energy for diffusion and NPL activation energy for viscosity are, within experimental error, almost identical, the results suggest that the ionic diffusivity is related strongly to the viscosity of the slag.

F. *Fluoride Addition*

The effect of calcium fluoride on $D_{e,Mn}$ values are shown in Table XII. In the first series of experiments, 1 pct CaF_2 was added to both capillary and crucible slag. Fluorine, when added as calcium fluoride, is a strong network modifier. Mills and Sridhar[11] determined the optical basicity coefficient of CaF_2 (Λ_i) to be 1.2 (*cf.* $\Lambda_{CaO} = 1.00$), thus making CaF_2 a strong network modifying species. Because optical basicity is directly related to slag viscosity, addition of CaF_2 to almost any slag will result in a decrease in viscosity. The amounts added experimentally were very small, only 1 pct by mass. This will lead to only a small decrease in slag viscosity, and a small increase in diffusivity, one that is negligible when experimental error is considered.

A second effect on slag properties that can be considered is electrical conductivity. Fluoride diffusivity is around a half order of magnitude greater than calcium.[3] The pres-

Table XII. Diffusivities of Manganese, with Fluoride Addition, in four-Component Systems with an Optical Basicity of 0.65 and Temperature of 1500 °C

	No CaF_2	1 Pct Uniform CaF_2	1 Pct CaF_2 Gradient
Optical Basicity	$D_{e,Mn}/(10^{-6}\ cm^2\ s^{-1})$	$D_{e,Mn}/(10^{-6}\ cm^2\ s^{-1})$	$D_{e,Mn}/(10^{-6}\ cm^2\ s^{-1})$
0.65	2.6 ± 0.4, 2.3 ± 0.3, 2.5 ± 0.4, 2.8 ± 0.5	2.5 ± 0.4, 2.2 ± 0.3	4.1 ± 0.6, 5.2 ± 0.8
0.61	1.5 ± 0.2, 1.4 ± 0.2, 1.4 ± 0.2	1.8 ± 0.3, 2.6 ± 0.4	2.8 ± 0.5, 2.3 ± 0.4
0.57	0.8 ± 0.1, 0.6 ± 0.1	0.5 ± 0.1, 0.4 ± 0.1	0.8 ± 0.1, 0.7 ± 0.1

ence of rapidly diffusing fluoride ions will increase electrical conductivity through an increase in ionic conduction. This can enhance multicomponent diffusion by minimizing cross-effects due to generation of regions of electric charge within the slag. Experimental results show a small increase in diffusivity with a fluoride gradient of zero. Although a small decrease in viscosity is created, the results can be attributed to an increase in electrical conductivity, allowing the reduction of cross-effects that reduce the diffusivity of manganese.

The second series of experiments involved addition of 1 pct CaF_2 to the crucible slag only, creating a fluoride concentration gradient in the same direction as manganese. Results showed a significant increase in diffusivity at all compositions, much greater than with a CaF_2 concentration gradient of zero. Viscosity effects will be even smaller for this regime, because fluoride is absent from the capillary slag prior to diffusion; however, a small viscosity decrease will be seen as fluoride diffuses along the capillary. The concentration gradient of fluoride creates diffusion of fluoride in the same direction as manganese. Fluoride diffuses rapidly, about 5 times that of manganese and calcium.[3] This will provide additional negative charge in the direction of manganese diffusion, acting as a driving force for the diffusion of manganese. The result is a marked increase in the overall diffusivity of manganese.

No analysis was performed to determine fluoride content in the slags before and after experimentation. While some fluoride loss undoubtedly occurred during slag preparation, the results indicate that some fluoride was still present in the slag, which accounted for the increase in diffusivity.

VI. CORRELATION BETWEEN DIFFUSIVITY AND OPTICAL BASICITY

The diffusion of ionic species through silicate slags is dependent on these main factors:

1. properties of the bulk slag medium, which can be characterized by such correlating properties as viscosity (η), molecular weight of silicate species, and basicity (*e.g.,* optical basicity, Λ);
2. interaction between oxygen and metal ions in the slag, which can be indicated by properties such as ion-oxygen attraction (I) and the optical basicity coefficient of diffusing species (Λ_i); and
3. temperature of system (T)—because Arrhenius behavior has been demonstrated, the model will account for compositional changes only.

Other minor factors, such as concentration dependence, do not significantly alter diffusivity compared with those points listed previously, and can be ignored. A semiempirical model can be developed from results obtained in this study that will predict diffusivity of metal cations through silicate slags at 1500 °C.

Because optical basicity is related directly to other properties such as slag viscosity and molecular size, a model for the estimation of diffusivity based on optical basicity can be formulated, in which optical basicity (Λ) is the variable and the optical basicity coefficient (Λ_i) is the parameter. A two-parameter exponential function can be optimized to fit the experimental data.

Introducing a silicon concentration gradient greatly alters diffusivity of cations. Determining a mathematical expression for the magnitude of D_{iSi} with changing basicity will enable incorporation of this factor into the overall model. Cross-effects from species other than silicon can be ignored. Because D_{iSi} is dependent on the interaction between species i and silicon, D_{iSi} will be a function of both Λ_i and Λ_{Si}, such that an increased value of Λ_i indicates a decreased interaction with silicon, and therefore a decreased D_{iSi}. The extent of this behavior is where $\Lambda_i \rightarrow \Lambda_{Si}$, in which case, $D_{iSi} \rightarrow D_{SiSi}$. The model is shown in Eq. [3].

$$D_{ij} = (9.3 \times 10^{-10}) \left(\frac{\Lambda_j^2}{\Lambda_i} \right) e^{12.5\Lambda} \qquad [3]$$

The condition on Eq. [1] is that j = Si, or j = i. This equation can calculate a multicomponent diffusion coefficient in a silicate system. Equation [3] gives the diffusivity at 1500 °C in $cm^2\ s^{-1}$ of D_{ii} or D_{iSi}, with a standard error of 15 pct. The overall diffusivity of any species can be determined simply by Fick's first law,[19] expanded for a multicomponent system, as shown in Eq. [4].

$$J_i = -\left(D_{ii} \frac{dC_i}{dx} + D_{iSi} \frac{dC_{Si}}{dx} \right) = -D_{e,i} \frac{dC_i}{dx} \qquad [4]$$

The term D_e denotes "effective diffusion coefficient," which is the experimentally measured diffusion coefficient.

The concentration gradient term dC/dx is calculated as the initial concentration difference of each oxide across the crucible/capillary junction, in terms of mole/gr. Figure 5 shows experimental and predicted diffusion coefficients for manganese. Data points are the reported effective diffusion coefficients. Fitted lines are effective diffusion coefficients, calculated using Eqs. [3] and [4], taking into account slag basicity and concentration gradients of all species. The oxidation state of manganese does not change significantly over the basicity range studied, and as such, there is no need to account for the different basicity of the Mn^{3+} species.

Figure 6 shows experimental and predicted diffusion coefficients for iron, for three- and five-component experiments.

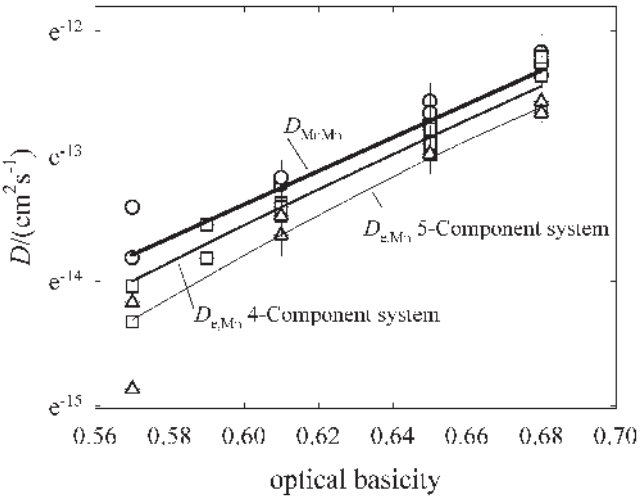

Fig. 5—Experimental diffusion coefficients of manganese in three- (O), four- ( ), and five- (△) component experiments at 1500 °C, showing D_{MnMn} and $D_{e,Mn}$ in the presence of two different silicon concentration gradients. Lines are predicted diffusivities, calculated using Eqs. [3] and [4].

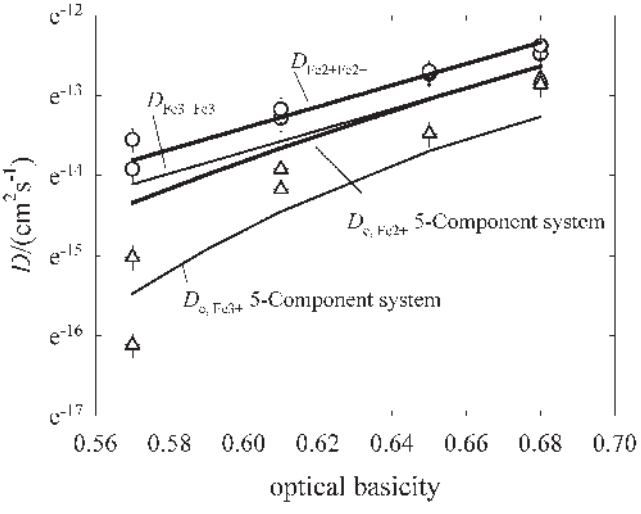

Fig. 6—Experimental diffusion coefficients for iron in three- (O) and five- (△) component experiments at 1500 °C, showing D_{FeFe} and $D_{e,Fe}$ in the presence of a silicon concentration gradient. The lines represent predicted diffusivities, calculated using Eqs. [3] and [4].

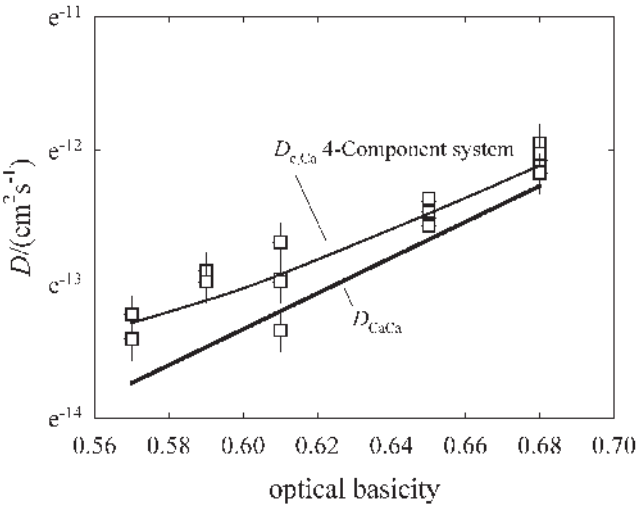

Fig. 7—Experimental diffusion coefficients of calcium, for four-component experiments at 1500 °C. The lines represent predicted diffusivities, calculated using Eqs. 3 and 4.

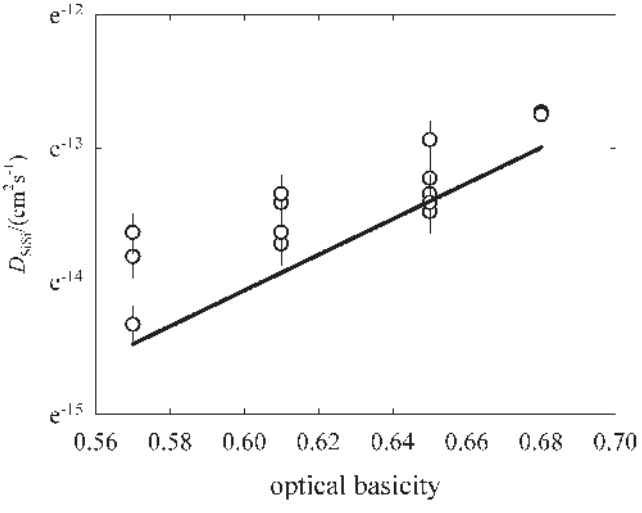

Fig. 8—Experimental diffusion coefficients of silicon at 1500 °C. The line represents predicted diffusivities, calculated using Eqs. [3] and [4].

The proportion of the Fe^{3+} ion increases exponentially with slag basicity, to a Fe^{3+}/Fe^{2+} of 0.6 at an optical basicity of 0.68. The heavier lines represent predicted diffusivity of the Fe^{2+} species, and the lighter line represents the Fe^{3+} species. The transformation of Fe^{2+} to Fe^{3+} is clearly predicted in the upper result set.

Figure 7 shows calculated and predicted diffusivities for calcium, determined for four-component experiments. Experimental data closely follow predicted values across the basicity range studied.

Figure 8 shows calculated and predicted diffusivities for silicon, determined for four- and five-component experiments. Obviously, silicon deserved different treatment than the metal cations, due to the incorporation of silicon in molecular networks. No cross-effects are assumed to act on silicon, due to the differences in ionic size. The statistical quality of the model when applied to silicon is poorer than for other species. Presentation of these data is for comparison only, but the fit of the data is still reasonable.

This model is semiempirical, based both on experimental data and physical constants, and allows for variation in slag basicity (as optical basicity) and the presence of a silicon concentration gradient. The model demonstrates the only significant cross-effect acting on the metal cations is a silicon concentration gradient. Experimental results show the model to provide a good estimate of multicomponent diffusion in silicate slags between optical basicity values of 0.57 and 0.68. This model gives good estimates of diffusion behavior of a variety of species in silicate slags of varying composition and temperature.

The fit of the model to the experimental cation diffusivity data is very good, particularly for manganese, for which

the most consistent experimental data were produced. The model fits variations in silicon concentration gradient very well, which confirms the finding that cross-effects induced by species other than silicon are negligible. The variation in diffusivity with varying Fe^{3+}/Fe^{2+} is clearly described. This of course depends on the accuracy of the determination of this ratio. The model consistently overestimates the diffusivity of iron against a silicon gradient, at all but the highest basicity. This could indicate that the iron-silicon interaction is not related to $\Lambda_{Si}/\Lambda_{Fe}$, or that the experimental data are inaccurate, or that the oxidation state in these experiments contained a greater proportion of Fe^{3+}. That the data lie between predicted lines for Fe^{3+} and Fe^{2+} suggests the latter could be the case.

Of the elements, the fit to the silicon data is the poorest, particularly at lower basicity. The model underestimates silicon diffusivity but the scatter in silicon microprobe concentration data in each experiment, due to the low molecular weight, makes the diffusivity of silicon the least reliable of the elements investigated. As silicon diffuses via a different mechanism to the metal cations, this difference is expected. Silicon is always present as silicate anions and is likely to diffuse in this state, as opposed to metal cations that are thought to diffuse through a series of jumps between nonbridging oxygen on silicate anions.

Results presented in this project support published optical basicity coefficients for transition metals. Taking into account the error inherent in any high-temperature experimental system, the coefficients of diffusion of Ca^{2+}, Mn^{2+}, Fe^{2+}, and Fe^{3+} are proportional to published optical basicity coefficients.[12] The variation in diffusivity of $Fe^{2+/3+}$ is an excellent illustration, strongly supporting published data. Optical basicity is an accurate constant of proportionality between the diffusivities of various species.

VII. DISCUSSION

The key factors that govern the diffusion of ionic species in molten slags have been identified. These factors can be divided into "solvent" properties (slag composition and molecular structure, temperature) and "solute" properties (network-forming ability, cross-effects between species).

A clear relationship is observed between molecular structure and diffusivity. The diffusivity of all species studied increased with a decrease in the average molecular size of the silicate anions present in the melt. As expected, the diffusivity of manganese increased with increasing temperature.

The diffusivities of individual species followed the trend $D_{CaCa} > D_{MnMn} \cdot D_{FeFe} > D_{SiSi}$. That silicon exhibited the lowest diffusivity is not surprising, because it exists only in the form of various silicate anions that are much larger than the cationic species. Manganese and iron exhibited similar diffusivities in acidic slags, but as basicity increased, iron diffusivity was relatively slower than manganese, mirroring the oxidation states of each species. In addition, the magnitude of the cross-effects with silicon followed the trend $D_{CaSi} < D_{MnSi} < D_{FeSi}$. These diffusion results suggest that the network forming ability of these species follows the trend $Ca^{2+} < Mn^{2+} < Fe^{2+} < Fe^{3+}$.

The observed correlation between optical basicity illustrates that the diffusion coefficients of the divalent cations Ca^{2+}, Mn^{2+}, and Fe^{2+} vary by only 10 pct. Variations in slag basicity from 0.57 to 0.68 cause an increase in the diffusion coefficient of Ca^{2+}, Mn^{2+}, and Fe^{2+} to increase by an order of magnitude. The silicate anion size is therefore by far the most significant factor in determining diffusion behavior.

The Stokes–Einstein relationship for condensed systems relates the diffusion coefficient of a solute to the solvent viscosity and radius of the solute.

$$D = \frac{k_B T}{6\pi\eta r} \quad [5]$$

Equation [5] applies where the solute species are much larger than the solvent species, where η is the viscosity of the medium, and r is the radius of the solute.[22] For the case where solvent and solute species are of a similar size, the 6 is replaced by a 4. For a given cation, the variation between diffusivity and the inverse of viscosity should be linear; however, the variation in the experimental diffusion coefficients with the inverse of viscosity, calculated using the NPL model, is nonlinear.

The coefficient of diffusion of a given solute in various media at various temperatures is inversely proportional to the solute radius. A decrease in ionic radius therefore will increase the diffusion coefficient. Ionic radii for the metal cations follow the trend $Ca^{2+} > Mn^{2+} > Fe^{2+} > Fe^{3+}$.[23] The Stokes–Einstein relation predicts that the diffusion coefficients will follow the trend $Fe^{3+} > Fe^{2+} > Mn^{2+} > Ca^{2+}$. The experimental diffusion coefficients show the opposite trend.

Molten slags are condensed systems rather than dilute, and the solvent molecules vary in size with changing composition. Diffusion in slags departs from these assumptions in that the solute ions ($Mn^{2+/3+}$, $Fe^{2+/3+}$, Ca^{2+}) are of a similar or smaller size than the solvent ions (complex silicate ions), and viscous flow is determined by large silicate anions. Furthermore, the charged nature of the solute and solvent molecules reduces the random nature of the diffusion. As such, the classical approach does not effectively describe the relationship between diffusion and viscosity in slag systems.

A further point of interest is comparison with previous diffusion studies. Several authors[3,6,24] reported iron to have diffusivities an order of magnitude greater than calcium. Keller and Schwerdtfeger[6] and Nowak and Schwerdtfeger[24] proposed the high diffusivity of iron was due to an interaction between the lone electron pair on bridging oxygen and the 3d orbital of Fe^{2+}. This reduces the jump energy for Fe^{2+} between non-bridging oxygen, and consequently enhances the rate of diffusion. Results presented here clearly show transition metals to have diffusivities slightly lower than calcium in identical systems, which follow accepted data on the network-forming ability of these ions, such as ion-oxygen attraction,[25] Pauling electronegativity,[12] and basicity index.[26]

ACKNOWLEDGMENTS

The authors thank Michael Haschke, Roentgenanalytik Messtechnik GmbH (Taunusstein, Germany), for assistance with X-ray probe analysis; Jorg Metz (La Trobe University) for assistance with electron probe analysis; Graeme Byrne (La Trobe University) for assistance with data modeling; and Oleg Ostrovski and Sean Gaal (University of New South Wales) for assistance with Raman analysis

REFERENCES

1. H. Towers, M. Paris, and J. Chipman: *J. Met.,* 1953, vol. 11, pp. 1455-88.
2. D.P. Argawal and D.P. Gaskell: *Metall. Mater. Trans. B,* 1975, vol. 6B (6), pp. 263-67.
3. R.F. Johnston, R.A. Stark, and J. Taylor: *Iron Steelmaking (Q.),* 1974, vol. 4 (4), pp. 220-27.
4. H. Keller, K. Schwerdtfeger, and K. Hennesen: *Metall. Mater. Trans. B,* 1979, vol. 10B, pp. 67-70.
5. H. Keller, K. Schwerdtfeger, H. Petri, R. Holze, and K. Hennesen: *Metall. Mater. Trans. B,* 1982, vol. 13B, pp. 237-40.
6. H. Keller and K. Schwerdtfeger: *Metall. Mater. Trans. B,* 1979, vol. 10B, pp. 551-54.
7. H. Shiraishi, H. Nagahama, and H. Ohta: *Can. Met. Q.,* 1983, vol. 22 (1), pp. 37-43.
8. H. Towers and J. Chipman: *J. Met.,* 1957, vol. 6, pp. 769-73.
9. P. Kubicek and T. Peprika: *Int. Met. Rev.,* 1983, vol. 28 (31), pp. 131-57.
10. J.A. Duffy and M.D. Ingram: *J. Am. Chem. Soc.,* 1971, vol. 93, pp. 6448-54.
11. K.C. Mills and S. Sridhar: *Iron Steelmaking,* 1999, vol. 26 (4), pp. 262-68.
12. I.D. Sommerville and Y. Yang: *Int. Conf. on Mineral Processing and Extractive Metallurgy,* AIMM, Melbourne, Australia, 2000.
13. D.J. Sosinsky and I.D. Sommerville: *Metall. Mater. Trans. B,* 1986, vol. 6B, pp. 405-09.
14. B.O. Myser, D. Virgo, and C.M. Scarfe: *Am. Mineralogist,* 1980, vol. 65, pp. 690-710.
15. S.A. Brawer and W.B. White: *J. Non-Cryst. Solids,* 1977, vol. 23, pp. 261-78.
16. M. Taylor and G.E. Brown: *Geochim. Cosmochim. Acta,* 1979, vol. 44, pp. 109-19.
17. E.T. Turkdogan: *Physicochemical Properties of Molten Slags and Glasses,* 1983, The Metals Society, London, 1983.
18. N. Sano and F. Tsukihashi: *6th Int. Conf. on Molten Slags, Fluxes and Salts,* Stockholm, Sweden, and KTH, Helsinki, Finland, 2000.
19. J. Crank: *The Mathematics of Diffusion,* 2nd ed., Clarendon Press, Oxford, United Kingdom, 1975.
20. V.H.J. Engell and P. Vygen: *Berichte der Bunsengesellschaft,* 1968, vol. 72 (1), pp. 5-12.
21. X. Lu, F. Li, L. Li, and K. Chou: in *6th Int. Conf. on Molten Slags, Fluxes and Salts,* Stockholm, Sweden, and, Helsinki, Finland, 2000.
22. H.J.V. Tyrrell and K.R. Harris: *Diffusion in Liquids—A Theoretical and Experimental Study,* Butterworth and Co., London, 1984.
23. *CRC Handbook of Chemistry and Physics,* 76th ed., D.R. Lide, ed., CRC Press, Boca Raton, FL, 2002.
24. N. Nowak and S. Schwerdtfeger: in *Metal-Gas-Slag Reactions and Processes,* Z.A. Fouroulis and W.W. Smeltzer, eds., The Electrochemical Society, Princeton, NJ, 1975, pp. 98-111.
25. J. Elliot, M. Glesier, and V. Ramakrishna: *Thermochemistry for Steelmaking,* Addison-Wesley, Reading, MA, 1963, vol. 2.
26. K.C. Mills: *The Slag Atlas,* Verlag Stahleisen GmbH, Dusseldorf, 1995, pp. 9-19.